Two-dimensional Excitonic Photoluminescence in Graphene on a Cu Surface

Youngsin Park,[†,‖] Yoo S. Kim,[‡,‖] Chang Woo Myung,[†,‖] Robert A. Taylor,[§] Christopher C. S. Chan,[§] Benjamin P. L. Reid,[§] Timothy J. Puchtler,[§] Robin J. Nicholas,[§] Tomba S. Laishram,[†] Geunsik Lee,[†] Chan C. Hwang,[⊥,*] Chong Yun Park,[‡,*] Kwang S. Kim[†,*]

[†]Center for Superfunctional Materials, Department of Chemistry and Department of Physics, Ulsan National Institute of Science and Technology (UNIST), Ulsan 44919, Korea

[‡]Department of Physics, Sungkyunkwan University, Suwon 16418, Korea

[§]Clarendon Laboratory, Department of Physics, University of Oxford, Parks Road, Oxford OX1 3PU, UK

[⊥]Beamline division, Pohang Accelerator Laboratory, Pohang 37673, Korea

[‖] These authors contributed equally to this work.

TOC Graphics

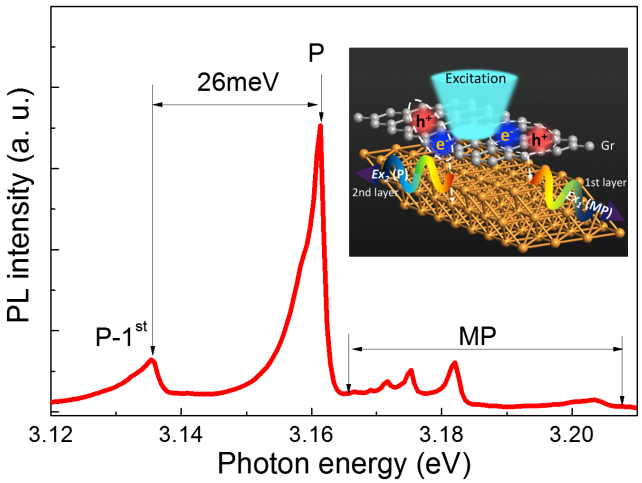

ABSTRACT

Despite having outstanding electrical properties, graphene is unsuitable for optical devices because of its zero band gap. Here, we report two-dimensional excitonic photoluminescence (PL) from graphene grown on a Cu(111) surface, which shows an unexpected and remarkably sharp strong emission near 3.16 eV (full-width at half-maximum $\leq$ 3meV) and multiple emissions around 3.18 eV. As temperature increases, these emissions blue-shift, displaying the characteristic negative thermal coefficient of graphene. The observed PL originates from the significantly suppressed dispersion of excited electrons in graphene caused by hybridization of graphene π and Cu d orbitals of the 1st and 2nd Cu layers at a shifted saddle point 0.525(M+K) of the Brillouin zone. This finding provides a new pathway to engineering novel optoelectronic graphene devices, whilst maintaining the outstanding electrical properties of graphene.

KEYWORDS: Exciton, Photoluminescence, Graphene, Optoelectronics, Cu surface

Graphene has been widely studied due to its remarkable electronic properties.[1-6] Nevertheless, because of its zero band gap, graphene has not been considered as a useful optical material.[6-11] Excited electron and hole pairs are easily screened by free electrons in metals. This makes the luminescence efficiency of metals very low such that only band to band transitions are significant, as observed in noble metals.[11] Surprisingly, excitonic features for metallic carbon nanotubes were predicted theoretically and observed in optical absorption experiments,[12-13] leading to possible enhancements in luminescence. These were explained by the fact that screening is not effective in one-dimensional metals. For 2-dimensional (2D) materials having intriguing 2D electronic features near the Fermi level like graphene, sharp luminescence is not observed. While an exciton in 2D semi-metallic graphene was predicted,[14-15] no direct experimental evidence has been reported despite the existence of some signatures.[16] Recent experiment showed broad light emission across the visible range (1.7-3.5 eV) in pristine monolayer graphene, where excited electrons are thermalized by optical phonons.[17] Here we show the excitonic photoluminescence (PL) of graphene on Cu, which reveals the presence of an exciton in the quasi 2D system, where Cu is unique in the sense that it interacts weakly with graphene so that the Dirac cone remains.

RESULTS AND DISCUSSION

Micro-photoluminescence (μ-PL) spectra of a graphene sheet synthesized on a Cu(111) surface measured at an arbitrary position is shown in Figure 1a. A strong and sharp PL peak near 3.161 eV (the lowest energy emission peak, denoted as P) and many peaks around 3.18 eV (denoted as MP) were observed. Figure 1b shows that no PL is visible in the range from 3.1 ~ 3.22 eV for a pristine Cu(111) surface and a cleaned Cu(111) surface in the CVD chamber, indicating that the PL in Figure 1a arises from the graphene grown on the substrate. Unlike the PL of

graphene quantum dots (GQDs) and graphene oxide (GO), which exhibit a broad luminescence,[18-20] very sharp PL emission features showing a full-width at half-maximum (FWHM) Γ of $\leq$ 3 meV were measured. These emissions have not been observed in ordinary graphene or GQDs. The asymmetric P peak can be resolved into two components by fitting with Gaussian functions. The two emission lines are reconstructed as shown in the inset of Figure 1a. The lower energy peak may originate from a phonon replica of the higher energy peak with a phonon energy shift of ~4 meV (discussed later). The experimental results are verified by density functional theory (DFT) and density functional perturbation theory (DFPT) calculations (discussed later). Apart from the above emissions, additional peaks near 3.135 eV (denoted as P-1st) and 3.109 eV (denoted as P-2nd) were observed. These peaks are identified as the 1st and 2nd phonon replicas of P with a phonon energy of ~26 meV (as discussed in Figures 4 and 5).

We can rule out the possibility that the emission originates from graphene oxide or impurities. Figure 2a shows the Raman spectrum of the graphene/Cu(111) measured at 10 K. The Raman G peak ~1582 cm^{-1} observed in the graphene on a Cu(111) indicates a negligible doping level[21] and there is no Raman peak related to graphene oxide. After subtracting the background, we obtain the intensity ratio of the 2D to G peaks (I_{2D}/I_G) of ~ 6.3, indicating monolayer formation, which is a slightly higher value compared to a previous reported value of ~4.[22] However, the value of I_{2D}/I_G decreases to about 3.25 at room temperature, which is consistent with previous work (Fig. S1). The inset depicts the Raman spectrum around the D mode, originating from lattice defects. Inset depicts the Raman spectrum around the D mode, originating from lattice defects. There is no distinct peak. For comparison, the Raman spectra of the graphene grown on Cu foils and then transferred onto SiO_2 with different growth pressure

were presented (Fig. 2b). Mono-, bi-, and even multilayer graphene can form on the Cu foils depending on the pressure in the growth chamber.[24,25] The confocal Raman intensity (I_{2D}/I_G) mapping image of the graphene grown on a Cu foil under the growth condition of 5 Torr confirms the presence of both mono- and bi-layer graphene (Fig. 2c. see the dark regions showing local bilayer formation). Moreover, from the photoemission spectroscopy the C 1*s* core level peak is very sharp with a FWHM of ~0.8 eV near 284.5 eV with no noticeable oxide-related peaks, such as graphene oxide, COOH, CO_2, and CuO in the C 1*s* and Cu 3*p* core level spectra (Fig. S2). Water molecules physisorbed on the surface in air seem to be mainly responsible for the O 1*s* peak observed in wider spectra taken with 630 eV.

To understand the origin of these peaks, we performed DFT calculations using the VASP suite[26] with local density approximations (see Method). We consider three possible stacking configurations, where graphene carbon atoms in a unit cell (A and B) sit on 1st and 2nd Cu layer atoms (tophcp), 1st and 3rd layer atoms (topfcc), and 2nd and 3rd layer atoms (hcpfcc). Geometry optimization for different stackings showed weak interaction of graphene with Cu, $d > 3.0$ Å, in agreement with the very weak interaction expected based on accurate *ab initio* calculations.[27] The overall band structure features remain consistent in various stacking configurations (Figure S3). Here, we use one of the stacking configurations, tophcp. The Dirac band (Figure 3) of graphene (red dots) is disrupted with a bandgap of 13.5 meV, which is calculated to be 20 meV according to DFT+U[28] and is n-doped compared to the pristine case (black line). Copper bands contain a dispersive *sp* conduction band and a flat *d* valence band (blue and green dots). Although graphene interacts with copper weakly, the graphene π^* band is significantly perturbed by Cu p_x near the M point of Brillouin zone (BZ). This produces a new van Hove singularity (vHs) with the flattened band near the mid-point of M-K at an energy of 1.1 eV, giving rise to an enhanced density of states (DOS) as shown in

the DOS plot on the right side of Figure 3. For the valence band, the top-most Cu d_{z^2} band (near -1.6 eV) shows a significant orbital hybridization (see the inset) with the π band of graphene, consistent with the literature,[29] and produces large DOS peaks. Such an enhanced DOS for electrons and holes is likely to support an emissive transition due to (i) a significant coupling between C π and Cu d_{z^2} orbitals, (ii) an optical selection rule, and (iii) an insignificant change in momentum (the direct transition). We calculated the transition probability $P(\omega) \propto A_{fi}\rho_f\rho_i$ $P(\omega) \propto A_{fi}\rho_f\rho_i$, where A_{fi} is the dipole transition matrix between initial and final states and $\rho_{i(f)}$ is the density of initial (final) state. The DFT result shows a peak with a transition energy at 2.7 eV, which corresponds to the expected emission energy of P (Figure S4). Small discrepancies in DFT-predicted energy gaps are generally expected.[30]

The possibility that lattice vibrations are responsible for the asymmetric P line and P replicas is investigated using DFPT and the PHONOPY package[31] for the phonon dispersion of graphene on 5 Cu(111) layers. The phonon dispersion (Fig. 4a) manifests a well-known feature of phonon softening of graphene ZO and LO branch induced by interfacial mixing (charge transfer) of graphene π orbital and metal *d* orbital.[32] However, because the softening of graphene Γ-LO mode is quite small, our Raman G band showed almost the same value as pristine graphene (Fig. 2). Although the orbital hybridization of graphene and Cu gives rise to the finite Γ-ZA energy, we observe no ZA/ZO splitting at K confirming no significant adsorption of graphene to Cu substrate.[33] Since the excitation energies of phonon replicas are ~ 10 meV, we further investigated the electron-phonon coupling of low energy modes with 9 Cu layers. These low energy modes are largely populated by Cu optical modes and graphene acoustic modes. We assumed that our observed PL is direct transition. The graphene DOS has a suppressed dispersion peak at 3.65 meV due to the orbital hybridization between the Cu

substrate and the carbon atoms[33] of the ZA mode near Γ (Fig. 4b). Furthermore, electronic structure calculations (Fig. 5a) show a large energy shift of C π^* upon modulation of Γ-ZA mode. Significant energy level shift from DFT calculations indicates a large electron-phonon coupling. Therefore, we conclude that the highly populated graphene Γ-ZA mode couples to the π^* band and produces an asymmetric P line composed of consecutive overlapping Gaussian peaks with a splitting of 3.65 meV. The coupling of the conduction band and graphene Γ-ZA mode demonstrates the origin of the linear increase in the FWHM with temperature (Fig. 6). On the other hand, the topmost Cu layer atoms the first layer Cu(1) and the second layer Cu(2), which lie in the low energy modes region (Fig. 4c), should also be responsible for the electronic structure of the Cu-graphene system. Amongst the low energy modes, the Cu(2) out-of-plane vibration mode Γ-SV2[34] has an energy of 30 meV which is comparable to the energy shift of 26 meV for the P replicas. Upon modulation of the Γ-SV2 (Fig. 5b) mode, the electronic energy level of Cu(2) d_{z^2} changes by a significant amount Δε. Therefore, P-1st and P-2nd are most probably Cu surface phonon emissions. Our conclusion is also consistent with the recent ultrafast PL experiment of strong electron optical phonon coupling in monolayer graphene.[17]

The PL spectra shift to higher energy with increasing temperature (Fig. 6). Similar emission peaks were observed for graphene grown on Cu foils, even in the case of low quality graphene (Figure S5). The integrated intensity of the MP emissions decreases linearly with temperature, while that of the P emission increases up to ~40 K and then decreases. Figure 6b shows both PL energy and FWHM for P and MP emissions as a function of temperature. This temperature dependent band gap variation is understood in terms of lattice dilation and electron-lattice interactions. Interestingly, the PL peaks shift to higher energy with increasing temperature, which is the opposite trend to other semiconducting materials. This is in

agreement with previous studies verifying a negative thermal coefficient for graphene.[35-37] The temperature dependence of the band-gap proposed by O'Donnell and Chen[38] takes into account the influence of phonons on the bandgap energy to obtain a better fit for semiconductors at lower temperatures. They considered the following equation:

$$E_g(T) = E_g(0) - S\langle E_{ph}\rangle\left[\coth\left(\langle E_{ph}\rangle/2k_BT\right) - 1\right],$$

where $\langle E_{ph}\rangle$ is an average phonon energy and *S* is a dimensionless coupling constant. The measured data are in good agreement with the aforementioned relationship at all measured temperatures (red solid lines). The fitting parameter for $\langle E_{ph}\rangle$ was found to be ~26 meV for the P emission. The FWHM of the P emission exhibits a small linear increase with temperature up to ~20 K, and then broadens more steeply as the temperature is increased further. The thermal broadening of the emission linewidth due to the exciton-phonon interaction can be expressed by the equation:

$$\Gamma(T) = \Gamma_0 + \sigma T + \gamma_{LO} \exp(-E_{LO}/k_BT),$$[39]

which is denoted as a black solid line in Figure 6b. Here Γ_0 is the temperature-independent inhomogeneous broadening; as $T \rightarrow 0$ K, Γ_0 is 2.9 meV for the P emission from the fit. The last two terms are related to the homogenous broadening due to exciton-phonon interactions. Here σ is the coupling coefficient between an exciton and an acoustic phonon, and γ_{LO} is the coefficient for coupling between an exciton and the longitudinal optical (LO) phonon. The best fitting parameter is σ = 313.6 μeV/K, much higher than the values reported usually for semiconductor materials with similar transition energies such as InGaN quantum dot (QD) (1.7 μeV/K),[37] CdSe nanosheets (9.8 μeV/K for 4 ML),[40] and GaN QD (0.8 μeV/K),[41] which means that the out-of-plane acoustic phonon dominates over optical phonons.

CONCLUSION

In conclusion, this work reports excitonic photoluminescence from a graphene sheet grown on Cu surface. Strong and sharp emission lines were clearly observed near 3.16 eV (P) and 3.18 eV (MP). These emissions shift to higher energy with increasing temperature, indicating a negative thermal coefficient for graphene. From DFT calculations, the orbital hybridization of graphene π and the Cu surface *d* orbitals is responsible for the large optical transition probability and the shift of saddle point M to 0.525(M+K) of BZ. Strong electron phonon couplings in graphene on a Cu(111) are observed from the replica PL spectra and temperature dependent FWHM of PL confirmed by DFT and DFPT calculations. The present results could be utilized for development of new optoelectronic devices.

METHODS

Sample preparation. Graphene was grown on a Cu single-crystal ($7\times7\times1$ mm^3) in a hot furnace consisting of a 25 mm ID quartz tube. The Cu single-crystal disc was first placed in the center of a horizontal quartz tube mounted inside a high temperature furnace, and the tube was then evacuated, back filled with hydrogen (H_2) and argon (Ar), and the process was repeated three times to remove the residual air completely from the quartz tube. H_2 (100 sccm) and Ar (200 sccm) were introduced as the carrier gas, when the furnace temperature reached 1050 °C. A Cu single-crystal was pre-annealed at 1050 °C for 30 min to remove the native Cu oxide layer in the H_2 and Ar atmosphere. Then, CH_4 (5 sccm) was flowed through the system. In order to know the relation of the PL with graphene, we also prepared a cleaned Cu(111) sample obtained after annealing without introducing the CH_4 gas. The growth pressure was set to 5 Torr during growth where monolayer graphene is formed. After exposure to CH_4, the

furnace was cooled to room temperature with H_2 and Ar. The experimental parameters (temperature profile and gas composition/flow rate) are in Figure S6.

X-ray Photoemission Spectroscopy. The core-level photoemission spectroscopy studies were performed at a pressure of 1.0×10^{-10} Torr at the 10D and 4A2 beamline of the Pohang Accelerator Laboratory (PAL), equipped with the PHOIBOS 150 and Scienta R4000 electron energy analyzers. All the spectra were collected at the normal emission. The photon energy used 360 eV to obtain high-quality C 1*s* core level spectra. The binding energy scale was calibrated with the Au 4*f* core-level peak at 84.0 eV.[42]

DFT calculations. For the plane wave DFT calculations, we used the local density approximation (LDA) exchange functional and a plane wave basis set with a 600 eV cut-off energy. We sampled the BZ with a (128×128×1) k-point mesh to calculate electronic structures such as the density of states. We used DFPT for phonon dispersion and a supercell method for the phonon DOS. We used a lattice constant of 2.46 Å for pristine graphene. The electronic coupling between the graphene and Cu(111) is weak, based on the ARPES experiments,[43-45] showing intact Dirac bands, and the theoretical calculations[29,46] predict a mean interlayer distance ~3.0 Å and a corrugation ~0.2 Å. Thus, we used a weakly interacting distance of 3 Å and a (1×1) unit cell after verifying the insignificant effects of stacking on the electronic band structure. The independent particle approximation (IPA) was used to compute the dipole transition matrix.

Photoluminescence. A frequency-tripled femtosecond Ti:sapphire laser (100 fs pulses at 76 MHz) operating at 266 nm was used to excite the graphene in the μ-PL experiments. The sample was mounted in a continuous-flow helium cryostat, allowing the temperature to be controlled accurately from 4.2 K to room temperature. A 36× reflecting objective was held by a sub-micron precision piezoelectric stage above the cryostat and used to focus the incident laser beam to a spot size of ~2 μm^2 and to collect the resulting luminescence. The luminescence was then directed to a spectrometer with a spectral resolution of ~700 μeV. The signal was finally detected using a cooled charge coupled device (CCD) detector. All the PL spectra were obtained by using a 0.3m focal length spectrometer with a 1200 gr/mm grating, except for the wide range PL measurements from the pristine and cleaned Cu(111), where a 300 gr/mm grating was used.

■ ASSOCIATED CONTENT

* Supporting Information

Photoemission spectroscopy of graphene grown on a Cu(111) surface measured at several different regions; DFT band structure of various stacking configurations; IPA DFT calculations; Photoluminescence of graphene grown on a Cu foil; TCVD setup with schematic diagram of graphene growth. This material is available free of charge via the Internet at http://pubs.acs.org.

■ AUTHOR INFORMATION

Corresponding Authors

*E-mail: cchwang@postech.ac.kr

*E-mail: cypark@skku.ac.kr

*E-mail: kimks@unist.ac.kr

ORCID

Kwang S. Kim: 0000-0002-6929-5359

Robert A. Taylor: 0000-0003-2578-9645

Author Contributions

Y.P., Y.S.K. and C.W.M. contributed equally to this work. C.Y.P. and C.C.H. designed the initial experiment. Y.S.K. and C.Y.P. prepared samples, measured the Raman, and analyzed. Y.P., C.C.S.C., B.P.L.R., T.J.P, R.A.T. and R.J.N. participated PL experiments and analyzed. Y.P., T.S.L. and C.C.H. performed XPS experiment and analyzed. C.W.M., G.L. and K.S.K. performed DFT calculations and interpreted the experiment with theoretical understanding. Y.P, C.C.H., C.W.M., R.A.T., G.L. and K.S.K. wrote the manuscript. C.C.H., C.Y.P. and K.S.K. supervised the project.

Notes

The authors declare no competing financial interest.

■ ACKNOWLEDGMENTS

This research was supported by Basic Science Research Program (2015R1D1A1A01058332), the SRC Center for Topological Matter (No. 2011-0030787), and National Honor Scientist Program (2010-0020414) through the National Research Foundation

of Korea (NRF). The experiments at PLS were supported in part by MSIP and POSTECH. Computation was supported by KISTI (KSC-2015-C3-059, KSC-2015-C3-061).

REFERENCES

(1) Liu, M.; Ulin-Avila, E.; Geng, B.; Zentgraf, T.; Ju, L.; Wang, F.; Zhang, X. A Graphene-based Broadband Optical Modulator. *Nature* **2011**, *474*, 64–67.

(2) Novoselov, K. S.; Falko, V. I.; Colombo, L.; Gellert, P. R.; Schwab, M. G.; Kim, K. A Roadmap for Graphene. *Nature* **2012**, *490*, 192–200.

(3) Grigorenko, N.; Polini, M.; Novoselov, K. S. Electrically Controlled One-way Photon Flow in Plasmonic Nanostructures. *Nat. Photonics* **2012**, *6*, 749–758.

(4) García de Abajo, F. J. Graphene Nanophotonics. *Science* **2013**, *339*, 917–918.

(5) Vakil, A.; Engheta, N. Transformation Optics Using Graphene. *Science* **2011**, *332*, 1291–1294.

(6) Geim, A. K. Graphene: Status and Prospects. *Science* **2004**, *324*, 1530-1534.

(7) Novoselov, K. S.; Geim, A. K.; Morozov, S. V.; Jiang, D.; Zhang, Y.; Dubonos, S. V.; Grigorieva, I. V.; Firsov, A. A. Electric Field Effect in Atomically Thin Carbon Films. *Science* **2004**, *306*, 666-669.

(8) Zhang, Y.; Tan, Y.; Stormer, H. L.; Kim, P. Experimental Observation of the Quantum Hall Effect and Berry's Phase in Graphene. *Nature* **2005**, *438*, 201-204.

(9) K. S. Novoselov, A. K. Geim, S. V. Morozov, D. jiang, M. I. Katsnelson, I. V. Grigorieva, S. V. Dubonos, A. A. Firsov, Two-dimensional Gas of Massless Dirac Fermions in Graphene. *Nature* **438**, 197-200 (2005)

(10) Geim, A. K.; Novoselov, K. S. The Rise of Graphene. *Nat. Mater.* **2007**, *6*, 183-191.

(11) Mooradian, A. Photoluminescence of Metals. *Phys. Rev. Lett.* **1969**, *22*, 185-187.

(12) Spataru, C. D.; Ismail-Beigi, S.; Benedict, L. X.; Louie, S. G. Excitonic Effects and Optical Spectra of Single-Walled Carbon Nanotubes. *Phys. Rev. Lett.* **2004**, *92*, 077402.

(13) Wang, F.; Cho, D. J.; Kessler, B.; Deslippe, J.; Schuck, P. J.; Louie, S. G.; Zettl, A.; Heinz, T. F.; Shen, Y. R. Observation of Excitons in One-Dimensional Metallic Single-Walled Carbon Nanotubes. *Phys. Rev. Lett.* **2007**, *99*, 227401.

(14) Yang, L.; Deslippe, J.; Park, C.-H.; Cohen, M. L.; Louie, S. G. Excitonic Effects on the Optical Response of Graphene and Bilayer Graphene. *Phys. Rev. Lett.* **2009**, *103*, 186802.

(15) Yang, L. Excitons in Intrinsic and Bilayer Graphene. *Phys. Rev. B* **2011**, *83*, 085405.

(16) Mak, K. F.; Shan, J.; Heinz, T. F. Seeing many-body Effects in Single- and Few-Layer Graphene: Observation of Two-Dimensional Saddle-Point Excitons. *Phys. Rev. Lett.* **2011**, *106*, 046401.

(17) Lui, C.H.; Mak, K. F.; Shan, J.; Heinz, T. F. Ultrafast Photoluminescence From Graphene. *Phys. Rev. Lett.* **2010**, *105*, 127404.

(18) Liu, F.; Jang, M.; Ha, H. D.; Kim, J.; Cho, Y.; Seo, T. S. Facile Synthetic Method for Pristine Graphene Quantum Dots and Graphene Oxide Quantum Dots: Origin of Blue and Green luminescence. *Adv. Matter.* **2013**, *25*, 3657-3662.

(19) Pan, D.; Zhang, J.; Li, Z.; Wu, M. Hydrothermal Route for Cutting Graphene Sheets into Blue-luminescent Graphene Quantum Dots. *Adv. Matter.* **2010**, *22*, 734-738.

(20) Kim, S.; Hwang, S. W.; Kim, M.; Shin, D. Y.; Shin, D. H.; Kim, C. O.; Yang, S. B.; Park, J. H.; Hwang, E.; Choi, S.; Ko, G.; Sim, S.; Sone, C.; Choi, H. J.; Bae, S.; Hong, B. H. Anomalous Behaviors of Visible Luminescence from Graphene Quantum Dots: Interplay between Size and Shape. *ACS Nano* **2012**, *6*, 8203-8208.

(21) Yan, J.; Zhang, Y.; Kim, P.; Pinczuk, A. Electric field Effect Tuning of Electron–Phonon Coupling in graphene. *Phys. Rev. Lett.* **2007**, *98*, 166802.

(22) Ferrari, A. C.; Meyer, J. C.; Scardaci, V.; Casiraghi, C.; Lazzeri, M.; Mauri, F.; Piscanec, S.; Jiang, D.; Novoselov, K. S.; Roth, S. Geim, A. K. Raman Spectrum of Graphene and Graphene Layers. *Phys. Rev. Lett.* **2006**, 97, 187401.

(23) Tu, Z.; Liu, Z.; Li, Y.; Yang, F.; Zhang, L.; Zhao, Z.; Xu, C.; Wu, S.; Liu, H.; Yang, H.; Richard, P. Controllable Growth of 1–7 Layers of Graphene by Chemical Vapour Deposition. *Carbon* **2014** 73, 252-258.

(24) Sun, Z.; Raji, A. O.; Zhu, Y.; Xiang, C.; Yan, Z.; Kittrell, C.; Samuel, E. L. G.; Tour, J. M. Large-Area Bernal-Stacked Bi-, Tri-, and Tetralayer Graphene. *ACS Nano* 2012*, 6*, 9790-9796.

(25) Song, W.; Jeon, C.; Kim, S. Y.; Kim, Y.; Kim, S. H.; Lee, S.; Jung, D. S.; Jung, M. W.; An, K.; Park, C. Two Selective Growth Modes for Graphene on a Cu Substrate Using Thermal Chemical Vapor Deposition. *Carbon* **2014**, *68*, 87-94.

(26) Kresse, G.; Furthmuller, J. Efficient Iterative Schemes for *ab initio* Total-Energy Calculations using a Plane-Wave Basis Set. *Phys. Rev. B* **1996**, *54*, 11169.

(27) Youn, I. S.; Kim, D. Y.; Singh, N. J.; Park, S. W.; Youn, J.; Kim, K. S. Intercalation of Transition Metals into Stacked Benzene Rings: A model Study of the Intercalation of Transition Metals into Bi-layered Graphene. *J. Chem. Theory Comput.* **2012**, *8*, 99-105.

(28) Frank, T.; Gmitra, M.; Fabian, J. Theory of Electronic and Spin-orbit Proximity Effects in Graphene on Cu(111). *Phys. Rev. B* **2016**, *93*, 155142.

(29) Vita, H.; Bottcher, S.; Horn, K.; Voloshina, E. N.; Ovcharenko, R. E.; Kampen, Th.; Thissen, A.; Dedkov, Yu. S. Understanding the Origin of Band Gap Formation in Graphene on Metals: Graphene on Cu/Ir(111). *Sci. Rep.* **2014**, *4*, 5704.

(30) Perdew, J. P. Density Functional Theory and the Band Gap Problem. *Int. J. Quant. Chem.* **1985**, *28*, 497.

(31) Togo, A.; Tanaka, I. First Principles Phonon Calculations in Material Science. *Scr. Matr.* **2015**, *108*, 1-5.

(32) Shikin, A. M.; Farias, D.; Rieder, K. H. Phonon Stiffening Induced by Copper Intercalation in Monolayer Graphite on Ni(111). *Europhys. Lett.* **1998**, *44*, 44-49.

(33) Allard, A.; Wirtz, L. Graphene on Metallic Substrates: Suppression of the Kohn Anomalies in the Phonon Dispersion. *Nano Lett.* **2010**, *10*, 4335–4340.

(34) Benedek, G.; Bernasconi, M.; Chis, V.; Chulkov, E.; Echenique, P. M.; Hellsing, B.; Toennies, J. P. Theory of Surface Phonons at Metal Surfaces: Recent Advances. *J. Phys.: Condens. Matter* **2010**, *22*, 084020.

(35) Mounet, N.; Marzari, N. First-principles Determination of the Structural, Vibrational and Thermodynamic Properties of Diamond, Graphite, and Derivatives. *Phys. Rev. B* **2005**, *71*, 205214.

(36) Jiang, J.-W.; Wang, J.-S.; Li, B. Thermal Expansion in Single-walled Carbon Nanotubes and Graphene: Nonequilibrium Green's Function Approach. *Phys. Rev. B* **2009**, *80*, 205429.

(37) Zakharchenko, K. V.; Katsnelson, M. I.; Fasolino, A. Finite Temperature Lattice Properties of Graphene Beyond the Quasiharmonic Approximation, *Phys. Rev. Lett.* **2009**, *102*, 046808.

(38) O'Donnell, K. P.; Chen, X. Temperature Dependence of Semiconductor Band Gaps. *Appl. Phys. Lett.* **1991**, *58*, 2924-2926.

(39) Seguin, R.; Rodt, S.; Strittmatter, A.; Reißmann, L.; Bartel, T.; Hoffmann, A.; Bimberg, D.; Hahn, E.; Gerthsen, D. Multi-Excitonic Complexes in Single InGaN Quantum Dots. *Appl. Phys. Lett.* **2004**, *84*, 4023-4025.

(40) Achtstein, A. W.; Schliwa, A.; Prudnikau, A.; Hardzei, M.; Artemyev, M. V.; Thomsen, C.; Woggon, U. Electronic Structure and Exciton-Phonon Interaction in Two-dimensional Colloidal CdSe Nanosheets. *Nano Lett.* **2012**, *12*, 3151-3157.

(41) Amloy, S.; Yu, K. H.; Karlsson, K. F.; Farivar, R.; Andersson, T. G.; Holtz, P. O. Size Dependent Biexciton Binding Energies in GaN quantum Dots. *Appl. Phys. Lett.* **2011**, *99*, 251903.

(42) Moulder, J. F.; Stickle, W. F.; Sobol, P. E.; Bomben, K. D. *Handbook of X-ray Photoelectron Spectroscopy,* Physical Electronics, Eden Prairie, MN, 1995; Vol. 93.

(43) Dedkov, Yu. S.; Shikin, A. M.; Adamchuk, V. K.; Molodtsov, S. L.; Laubschat, C.; Bauer, A.; Kaindl, G. Intercalation of Copper Underneath a Monolayer of Graphite on Ni(111). *Phys. Rev. B* **2001**, *64*, 035405.

(44) González-Herrero, H.; Pou, P.; Lobo-Checa, J.; Fernández-Torre, D.; Craes, F.; Martínez-Galera, A. J.; Ugeda, M. M.; Corso, M.; Ortega, J. E.; Gómez-Rodríguez, J. M.; Pérez, R.; Brihuega, I. Graphene Tunable Transparency to Tunneling Electrons: A Direct Tool to Measure the Local Coupling. *ACS Nano* **2016**, *10*, 5131-5144.

(45) Dedkov, Yu. S.; Voloshina, E. Graphene Growth and Properties on Metal Substrates. *J. Phys.: Condens. Matter* **2015**, *27*, 303002.

(46) Voloshina, E. N.; Dedkov, Yu. S. General Approach to Understanding the Electronic Structure of Graphene on Metals. *Mater. Res. Express* **2014**, *1*, 035603.

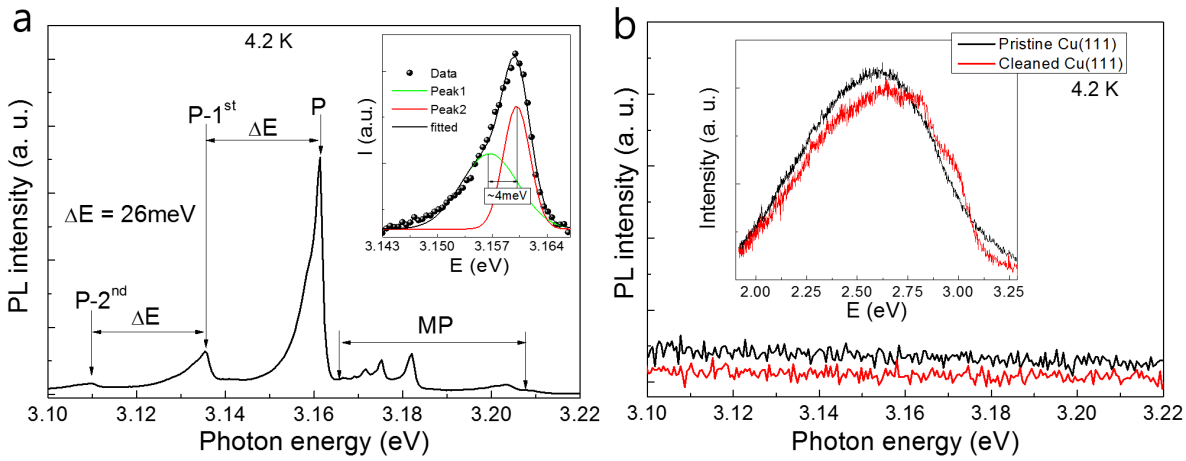

Figure 1. (a) Micro-PL spectrum of graphene grown on a Cu (111) surface measured at an arbitrary position at 4.2K. Inset depicts the reconstructed PL spectrum for the P emission using two Gaussian functions. (b) Micro-PL spectra of a pristine and a cleaned Cu(111) surface by annealing the surface in the CVD chamber prior to grow the graphene. Inset shows wide micro-PL spectra of these samples.

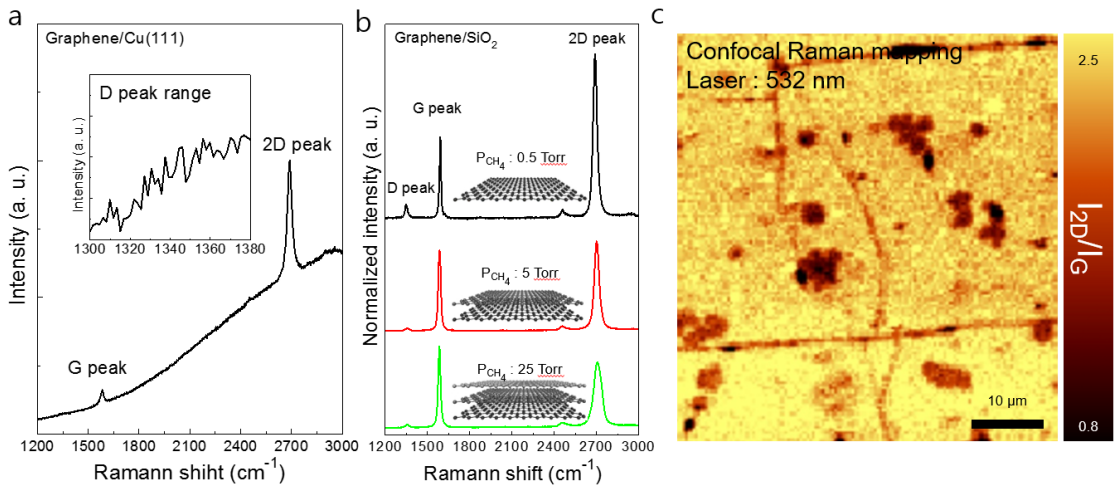

Figure 2. (a) Raman spectrum of the graphene grown on a Cu(111) single crystal without transferring. Inset depicts the Raman spectrum around the D mode. (b) Raman spectra of the graphene grown on Cu foils and then transferred onto SiO_2 with different growth pressure. (c) Confocal Raman intensity (I_{2D}/I_G) mapping image of the graphene grown on a Cu foil under the growth condition of 5 Torr.

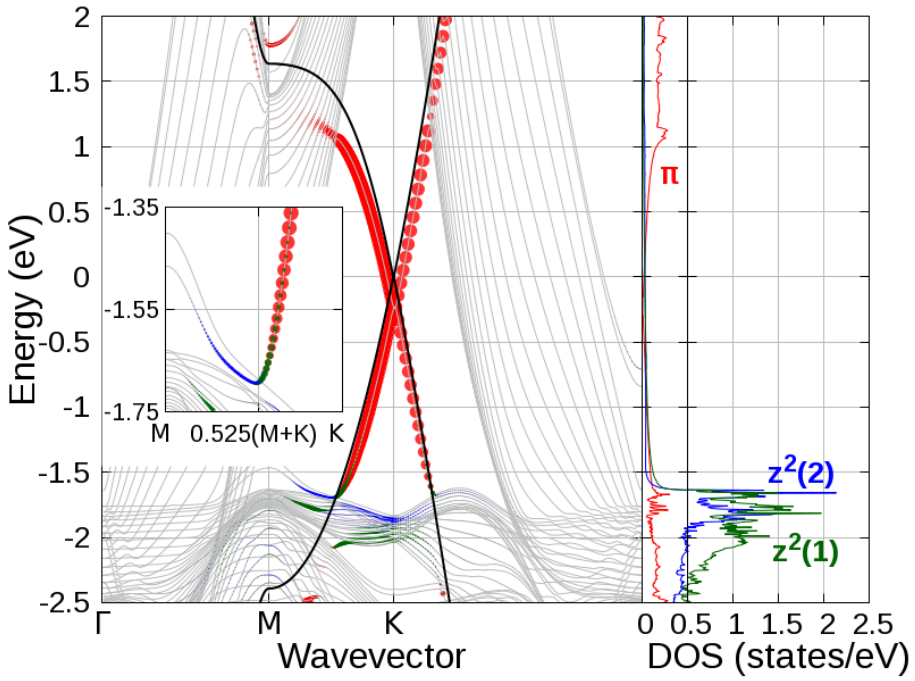

Figure 3. Band structure and projected DOS for 21-layer Cu (111)-graphene. Graphene π (red), first layer Cu(1) d_{z^2} (green), second layer Cu(2) d_{z^2} (blue), and pristine graphene (black). An enlarged band structure around the vHs at 0.525 (M+K) in the valence band is shown in the inset.

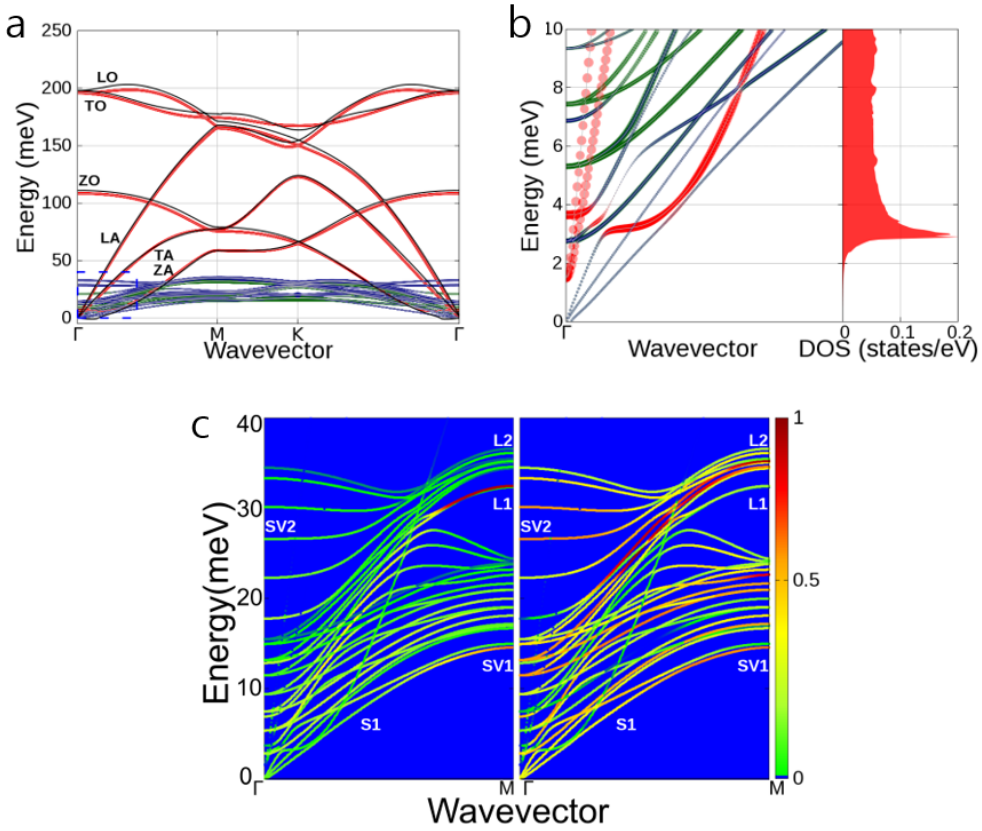

Figure 4. (a) Dynamical matrix projected phonon dispersion and phonon DOS of 5-layer Cu (111)-graphene, pristine graphene (black), graphene (red), the first Cu layer (green), and the second layer Cu (blue). Dashed blue box indicates low energy modes that are related to electron-phonon coupling. (b) Phonon dispersion and phonon DOS of low energy graphene modes of 9-layer Cu(111) graphene. (c) Normalized dynamical matrix projected phonon dispersion of 9-layer Cu(111) graphene for the first (left) and second (right) Cu layers near Γ. Surface Cu phonons consist of shear vertical (SV) and longitudinal (L) modes of the first (1) and the second (2) layer Cu atoms.[34]

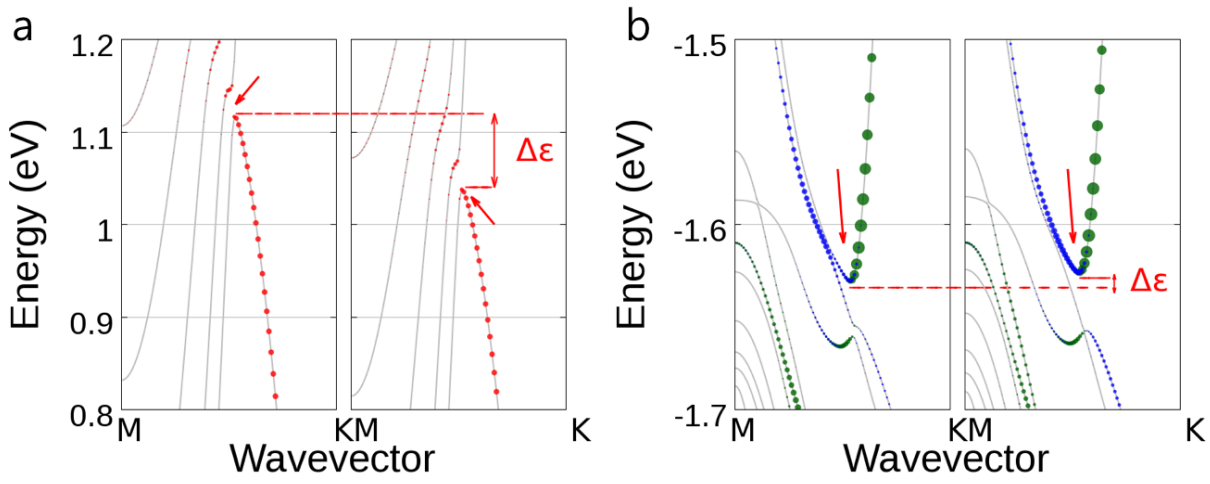

Figure 5. Indication of electron-phonon coupling between the graphene ZA and Cu SV2 mode. (a) Original band structure (left) and modified band structure (right) upon modulation of the ZA (3.56 meV) mode. (b) Original band structure (left) and modified band structure (right) upon modulation of the SV2 (30 meV) mode. Here, modulations are arbitrary so that energy shifts do not correspond to phonon energies.

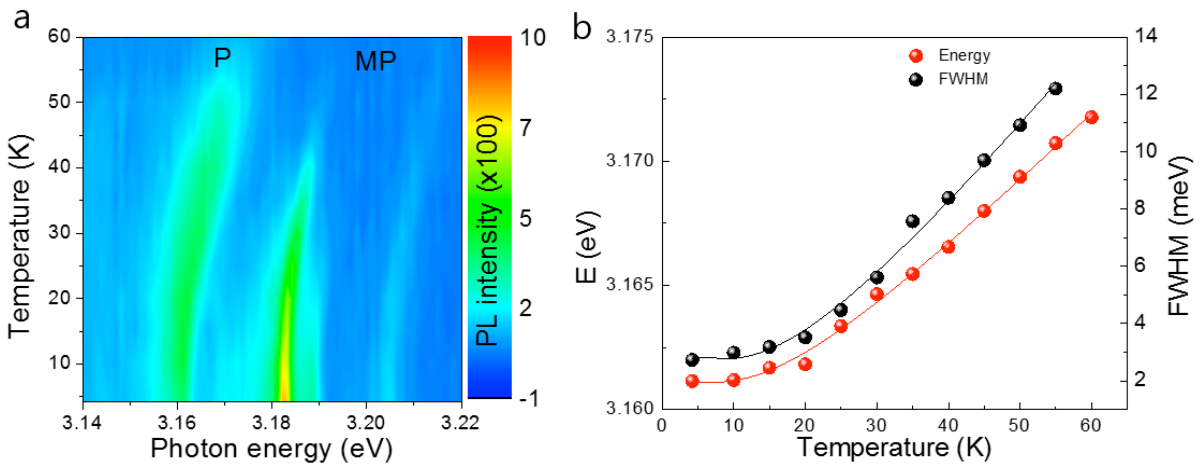

Figure 6. (a) Temperature-dependent micro-photoluminescence spectra of the graphene measured at an arbitrary region. (b) PL peak energy and full width at half maximum for the P peak as a function of temperature. The solid lines are the least square fitted curves.